Synthesis and Unexpected Electrochemical Behavior of the Triphenylamine-Based Aramids with *Ortho*- and *Para*-Trimethyl-Protective Substituents

HUNG-JU YEN, SHIUE-MING GUO, GUEY-SHENG LIOU

Functional Polymeric Materials Laboratory, Institute of Polymer Science and Engineering, National Taiwan University, No. 1, Sec. 4, Roosevelt Rd., Taipei 10617, Taiwan

Received 10 July 2010; accepted 18 August 2010
DOI: 10.1002/pola.24326
Published online 24 September 2010 in Wiley Online Library (wileyonlinelibrary.com).

ABSTRACT: Two series of new organosoluble polyamides with methyl-substituted triphenylamine (MeTPA) units showing anodically electrochromic characteristic were prepared from the phosphorylation polyamidation reaction of two diamine monomers, 4,4′-diamino-2″,4″,6″-trimethyltriphenylamine (Me_3TPA-diamine; **2**) and 4,4′-diamino-4″-methyltriphenylamine (MeTPA-diamine; **2′**), with various dicarboxylic acids, respectively. These polymers were readily soluble in many polar solvents and showed useful levels of thermal stability associated with relatively high glass-transition temperatures (T_g) (314–329 °C) and high char yields (higher than 62% at 800 °C in nitrogen). In addition, the polymer films showed reversible electrochemical oxidation, high coloration efficiency (CE), low switching time, and anodic green electrochromic behavior. The unexpected electrochemical behavior of higher oxidation potential and lower electrochemical stability of Me_3TPA-polyamides **I** than MeTPA corresponding polymers could be attributed to the higher steric hindrance of ortho-substituents in Me_3TPA moieties, thus made the resonance stabilization of cation radical much more difficult for the Me_3-substituted phenyl ring. © 2010 Wiley Periodicals, Inc. J Polym Sci Part A: Polym Chem 48: 5271–5281, 2010

KEYWORDS: electrochemistry; high performance polymers; UV–vis spectroscopy; polyamides

INTRODUCTION Electrochromic materials can be defined as one where the reversible color change takes place from electrochemically induced redox states. Color changes are commonly between a transparent state, where the chromophore only absorbs in the ultraviolet (UV) region, and a colored state which absorbs in the visible even near-infrared range in a given electrolyte solution. Recently, the application of electrochromic materials, such as antiglare back mirrors, smart windows, and E-papers, have already been commercialized nowadays.[1–3] In general, most applications require electrochromic materials with a high contrast ratio ($\Delta T\%$), coloration efficiency (CE),[4] cycle life, and rapid response time.

Wholly aromatic polyamides are known as highly thermally stable materials, with a favorable balance of physical and chemical properties. However, rigidity of the backbone and strong hydrogen bonding result in high melting or glass-transition temperatures (T_g) and limited solubility in most organic solvents.[5,6] These properties make them difficult to process, thus restricting their applications. To overcome such a dilemma, introduction of bulky and packing-disruptive groups into the polymer backbone is a feasible approach[7–14]; triphenylamine (TPA) derivatives provide an avenue. Since 2002, we have developed TPA containing polyamides and polyimides as high-performance polymers and hole-transporting materials.[15–18]

The anodic oxidation pathways of TPA were well studied.[19] The electrogenerated cation radical of TPA is not stable and the radical electron could resonance to ortho and para position. The chemical follow-up reaction produced tetraphenylbenzidine (TPB) by tail-to-tail coupling and the loss of two protons per dimer. When the phenyl groups have substituents at the para position, the coupling reactions are greatly prevented. It has been well established that incorporation of electron-donating substituents at the para positions of triarylamines affords stable radical cations.[20,21]

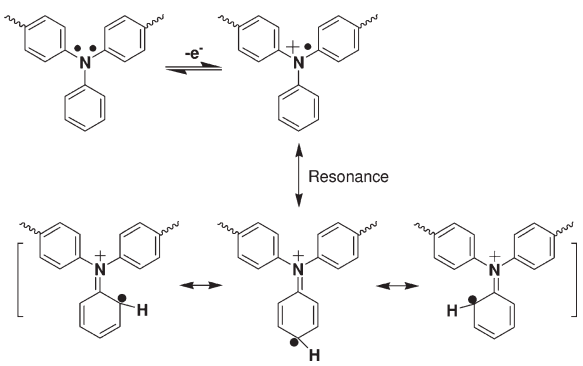

In addition to para coupling of TPA, ortho coupling can also take place.[22] In this article, we, therefore, synthesized a

Additional Supporting Information may be found in the online version of this article. Correspondence to: G.-S. Liou (E-mail: gsliou@ntu.edu.tw)
Journal of Polymer Science: Part A: Polymer Chemistry, Vol. 48, 5271–5281 (2010)

novel diamine, 4,4′-diamino-2″,4″,6″-trimethyltriphenylamine (Me_3TPA-diamine; **2**), and its derived polyamides containing Me_3TPA groups to investigate the electrochemical behavior and the substituent effect on the electrochromic stability and redox potential of the resultant polymers. The general properties such as solubility and thermal properties are described. For a comparative study, electrochemical and electrochromic properties of the present polyamides were also compared with that of structurally related ones from 4,4′-diamino-4″-methyltriphenylamine (MeTPA-diamine; **2′**)[23] and 4,4′-diaminotriphenylamine (**2″**).[24]

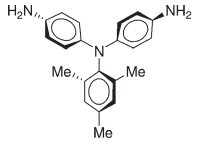

2

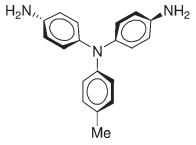

2′

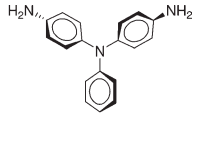

2″

EXPERIMENTAL

Materials

4,4′-Diamino-4″-methyltriphenylamine (**2′**, mp = 145–146 °C) was synthesized by hydrazine Pd/C-catalyzed reduction of 4,4′-dinitro-4″-methyltriphenylamine according to a previously reported procedure.[23] Commercially available dicarboxylic acids such as *trans*-1,4-cyclohexanedicarboxylic acid (**3a**), 4,4′-oxydibenzoic acid (**3b**), and 2,2′-bis(4-carboxyphenyl)hexafluoropropane (**3c**) were purchased from Tokyo Chemical Industry and used as received. Anhydrous calcium chloride ($CaCl_2$) was dried under vacuum at 180 °C for 8 h. Tetrabutylammonium perchlorate (TBAP) was obtained from ACROS and recrystallized twice by ethyl acetate under nitrogen atmosphere and then dried *in vacuo* before use. All other reagents were used as received from commercial sources.

Polymer Synthesis

The synthesis of polyamide **Ib** was used as an example to illustrate the general synthetic route used to produce the polyamides. A mixture of 380.9 mg (1.20 mmol) of the diamine monomer (**2**), 310.9 mg (1.20 mmol) of 4,4′-oxydibenzoic acid (**3b**), 110.0 mg of calcium chloride, 1.00 mL of triphenyl phosphite, 0.50 mL of pyridine, and 1.00 mL of *N*-methyl-2-pyrrolidinone (NMP) was heated with stirring at 105 °C for 3 h. The obtained polymer solution was poured slowly into 300 mL of stirred water giving rise to a stringy, fiber-like precipitate that was collected by filtration, washed thoroughly with hot water and methanol, and dried under vacuum at 100 °C; yield: 0.646 g (99%). Reprecipitations of the polymer by *N,N*-dimethylacetamide (DMAc)/methanol were carried out twice for further purification. The inherent viscosity and weight-average molecular weights (M_w) of the obtained polyamide **Ib** was 0.68 dL/g (measured at a concentration of 0.5 g/dL in DMAc at 30 °C) and 151,900 daltons, respectively. The FT-IR spectrum of **Ib** (film) exhibited characteristic amide absorption bands at 3312 cm^{-1} (*N*—H stretch), 3040 cm^{-1} (aromatic C—H stretch), 2917, 2854 cm^{-1} (CH_3 C—H stretch), 1650 cm^{-1} (amide carbonyl), 1233 cm^{-1} (asymmetric stretch C—O—C), and 1012 cm^{-1} (symmetric stretch C—O—C).

^{1}H-NMR (500 MHz, DMSO-d_6, δ, ppm): 10.12 (s, 2H), 8.03 (d, J = 8.5 Hz, 4H), 7.61 (d, J = 8.5 Hz, 4H), 7.19 (d, J = 8.5 Hz, 4H), 7.01 (s, 2H), 6.85 (d, J = 8.5 Hz, 4H), 2.22 (s, 3H), 1.98 (s, 6H). Anal. Calcd. (%) for $(C_{35}H_{29}N_3O_3)_n$ $(539.62)_n$: C, 77.90%; H, 5.42%; N, 7.79%. Found: C, 75.52%; H, 5.06%; N, 7.02%. The other polyamides were prepared by an analogous procedure.

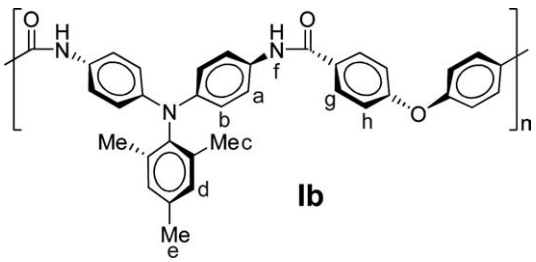

Ib

Preparation of the Film

A solution of polymer was made by dissolving about 0.65 g of the polyamide sample in 15 mL of DMAc. The homogeneous solution was poured into a 9-cm glass Petri dish, which was placed in a 90 °C oven for 5 h to remove most of the solvent; then the semidried film was further dried *in vacuo* at 160 °C for 8 h. The obtained films were ~65–80 μm in thickness and were used for solubility tests and thermal analyses.

Measurements

Fourier transform infrared (FT-IR) spectra were recorded on a PerkinElmer Spectrum 100 Model FT-IR spectrometer. Elemental analyses were run in a Heraeus VarioEL-III CHNS elemental analyzer. ^{1}H-NMR spectra were measured on a Bruker AVANCE-500 FT-NMR using tetramethylsilane as the internal standard, and peak multiplicity was reported as follows: s, singlet; d, doublet. X-Ray single-crystal diffraction experiments were carried on a Norius Kappa CCD four-circle diffractometer equipped with graphite-monochromated Mo-Kα radiation. The structures were solved by direct methods using SHELXL-97 software (Sheldrick, 1997). Wide-angle X-ray diffraction (WAXD) measurements were performed at room temperature (*ca.* 25 °C) on a Shimadzu XRD-7000 X-ray diffractometer (40 kV, 20 mA), using graphite-monochromatized Cu-Kα radiation. The inherent viscosities were determined at 0.5 g/dL concentration using Tamson TV-2000 viscometer at 30 °C. Gel permeation chromatographic (GPC) analysis was performed on a Lab Alliance RI2000 instrument (one column, MIXED-D from Polymer Laboratories) connected with one refractive index detector from Schambeck SFD Gmbh. All GPC analyses were performed using a polymer/*N,N*-dimethylformamide (DMF) solution at a flow rate of 1 mL/min at 70 °C and calibrated with polystyrene

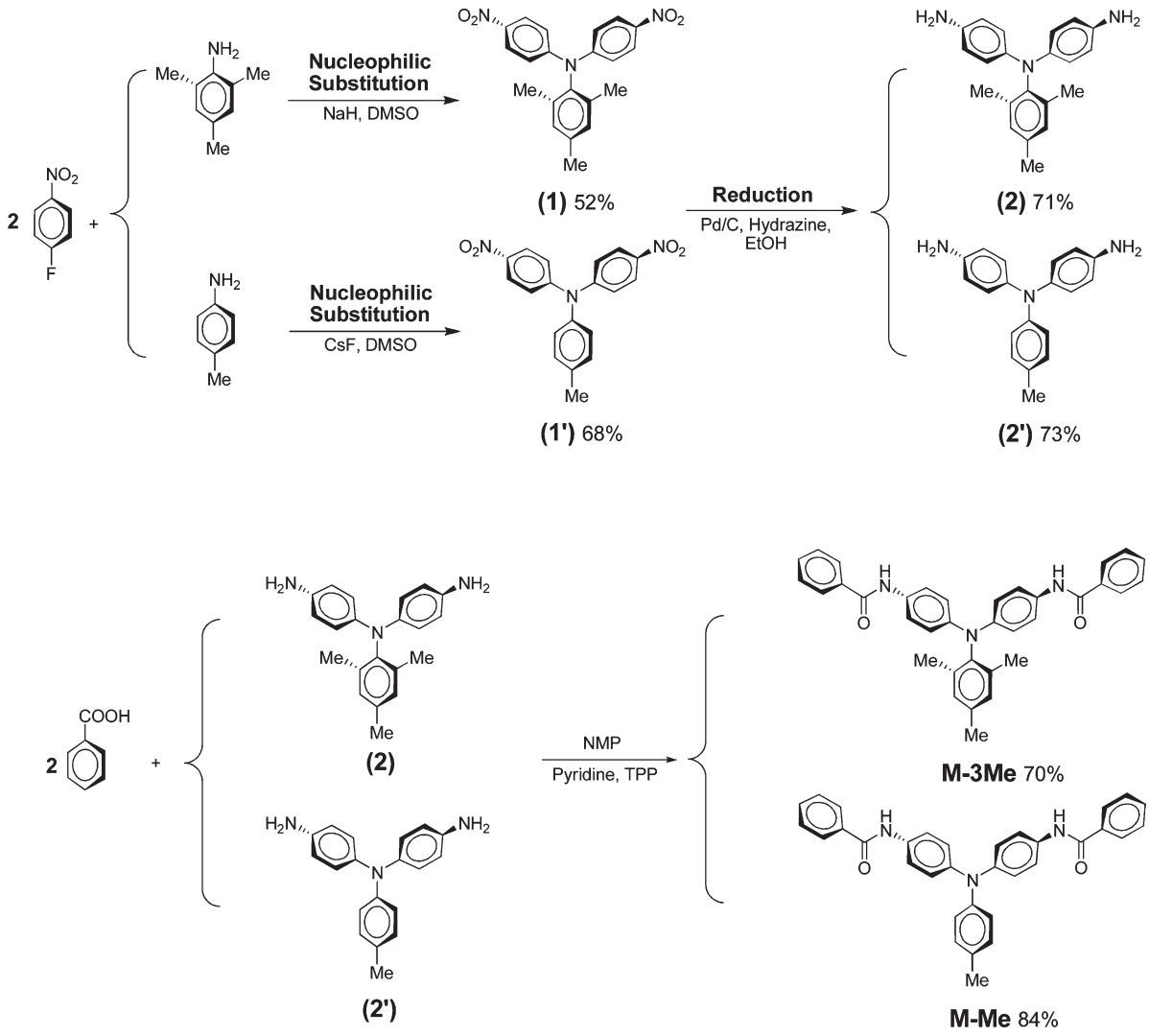

SCHEME 1 Synthetic routes for diamine monomers **2** and **2′**, and model compounds **M-3Me** and **M-Me**.

standards. Thermogravimetric analysis (TGA) was conducted with a PerkinElmer Pyris 1 TGA. Experiments were carried out on ~6–8-mg film samples heated in flowing nitrogen or air (flow rate = 20 cm^3/min) at a heating rate of 20 °C/min. DSC analyses were performed on a PerkinElmer Pyris 1 DSC at a scan rate of 10 °C/min in flowing nitrogen (20 cm^3/min). Electrochemistry was performed with a CH Instruments 611B electrochemical analyzer. Voltammograms are presented with the positive potential pointing to the left and with increasing anodic currents pointing downwards. Cyclic voltammetry (CV) was conducted with the use of a three-electrode cell in which indium-tin oxide (ITO, area of polymer films ~0.5 × 1.1 cm^2) was used as a working electrode. A platinum wire was used as an auxiliary electrode. All cell potentials were taken by using a homemade Ag/AgCl, KCl (sat.) reference electrode. Spectroelectrochemical experiments were carried out in a cell built from a 1-cm commercial UV-visible cuvette using Hewlett–Packard 8453 UV–vis diode-array spectrophotometer. The ITO-coated glass slide was used as the working electrode, a platinum wire as the counter electrode, and a Ag/AgCl cell as the reference electrode. CE (η) determines the amount of optical density change (δOD) at a specific absorption wavelength induced as a function of the injected/ejected charge (Q; also termed as electroactivity), which is determined from the *in situ* experiments. CE is given by the equation: $\eta = \delta OD/Q = \log[T_b/T_c]/Q$, where η (cm^2/C) is the CE at a given wavelength, and T_b and T_c are the bleached and colored transmittance values, respectively. The thickness of the polyamide thin films was measured by α-step profilometer (Surfcorder ET3000, Kosaka Lab., Japan).

RESULTS AND DISCUSSION

Monomer Synthesis

The new monomer Me_3TPA-diamine (**2**) was synthesized by hydrazine Pd/C-catalyzed reduction of the dinitro compound (**1**) resulting from the sodium hydride-mediated aromatic nucleophilic substitution reaction of 2,4,6-trimethylaniline with 4-fluoronitrobenzene (Scheme 1). Elemental analysis,

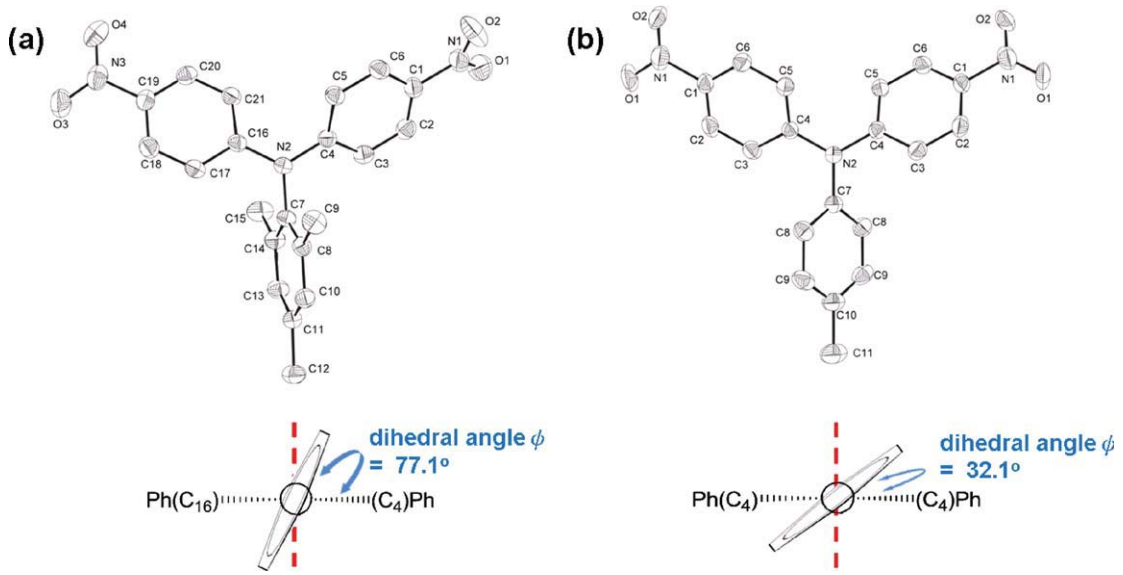

FIGURE 1 X-ray structures of dinitro compounds (a) **1** and (b) **1′**. [Color figure can be viewed in the online issue, which is available at wileyonlinelibrary.com.]

FT-IR, and NMR spectroscopic techniques were used to identify structures of the intermediate dinitro compound (**1**) and the targeted diamine monomer (**2**). The FT-IR spectra of these two synthesized compounds are illustrated in Figure S1 in Supporting Information. The nitro groups of compound (**1**) exhibited two characteristic absorption bands at around 1578 and 1307 cm^{-1} due to NO_2 asymmetric and symmetric stretching. After reduction to diamine monomer (**2**), the characteristic absorption bands of the nitro group disappeared and the primary amino group showed the typical absorption pair at 3401 and 3326 cm^{-1} (N—H stretching).

^1H and ^{13}C NMR spectra of the dinitro compound (**1**) and diamine monomer (**2**) are illustrated in Figure S2 and Figure S3, respectively, and agree well with the proposed molecular structures. The molecular structures of compounds (**1**) and (**1′**) were further confirmed by single-crystal X-ray diffraction (Fig. 1). The single crystal of (**1**) was acquired by slow crystallization of a DMF solution. As shown in Figure 1, the molecular structures both display a propeller-shaped conformation of the TPA core. Notably, the twist of N_2—C_7 bond in *ortho*-methyl-substituted compound **1** was more than that in compound **1′** due to the steric hindrance of *ortho*-dimethyl-substituents on the phenyl ring. The dihedral angle of the *ortho*-dimethyl-substituted phenyl ring in TPA core is about 77.1°. The model compounds **M-3Me** and **M-Me** were prepared from the condensation of diamine **2** and **2′** with two equivalent amounts of benzoic acid as shown in Scheme 1, and their IR spectroscopic data can be found in the ESI (Figure S4).

Polymer Synthesis

According to the phosphorylation technique described by Yamazaki,[25,26] two series of new polyamides **I** and **II** with main-chain Me_3TPA and MeTPA units were synthesized from the diamine monomers **2** and **2′** with three dicarboxylic acids (**3a–3c**), respectively, (Scheme 2). The polymerization was carried out via solution polycondensation using triphenyl phosphite and pyridine as condensing agents. All polymerization reactions proceeded homogeneously and gave high molecular weights. The obtained polyamides had inherent viscosities in the range of 0.40–1.41 dL/g with weight-average molecular weights (M_w) and polydispersity (PDI) of 44,700–151,900 daltons and 1.49–2.12, respectively, relative to polystyrene standards (Table S1). All the high molecular weights polymers could afford transparent and tough films via solution casting. The structures of the polyamides were confirmed by IR spectroscopy. As shown in Figure S5, a typical IR spectrum for polyamide **Ib** exhibited characteristic absorption bands of the amide group at around 3312 cm^{-1} (*N*—H stretch) and 1650 cm^{-1} (amide carbonyl). A structurally related polyamide **IIIb** derived from diamine **2″** is used for comparison, and the preparation of polymer **IIIb** has been described previously.[27]

Basic Characterization

The solubility properties of polymers **I** and **II** were investigated qualitatively, and the results are also listed in Table S2. Most of the polyamides were readily soluble in polar aprotic organic solvents, such as NMP, DMAc, DMF, dimethyl sulfoxide (DMSO), and *m*-cresol. Thus, the excellent solubility makes these polymers as potential candidates for practical applications by spin-coating or inkjet-printing processes to afford high-quality thin films for optoelectronic devices. The WAXD patterns of the polyamides given in Figure S6 indicated that the polymers were essentially amorphous. Their high solubility and amorphous properties can be attributed to the incorporation of bulky and noncoplanar Me_3TPA moiety along the polymer backbone, which results in a high steric hindrance for close packing and thus reduces their crystallization tendency.

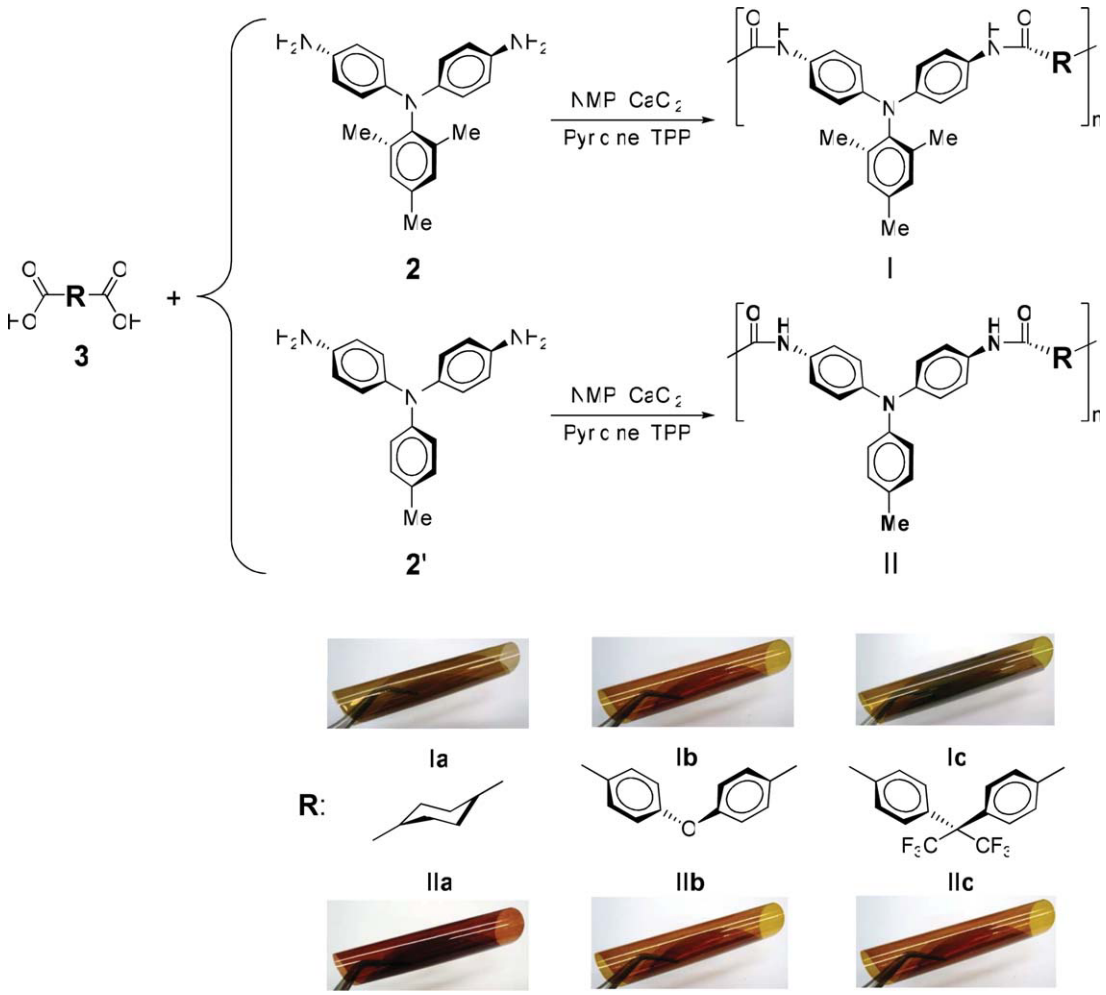

SCHEME 2 Synthesis of aromatic polyamides **Ia-Ic** and **IIa-IIc**. The photographs show appearance of the flexible films (thickness: 65–80 μm). [Color figure can be viewed in the online issue, which is available at wileyonlinelibrary.com.]

The thermal properties of polyamides were examined by TGA and DSC, and the thermal behavior data are summarized in Table S3. Typical TGA curves of polyamide **Ic** and **IIc** are shown in Figure S7. All the prepared polyamides exhibited good thermal stability with insignificant weight loss up to 450 °C under nitrogen or air atmosphere. The 10% weight loss temperatures of these polymers in nitrogen and air were recorded in the range of 450–535 and 460–540 °C, respectively. The concentration of carbonized residue (char yield) of these polymers in a nitrogen atmosphere was more than 62% at 800 °C. The high char yields of these polymers can be ascribed to their high aromatic content. The glass-transition temperatures (T_g) of polyamides **I** and **II** could be easily measured by the DSC thermograms; they were observed in the range of 314–329 and 293–313 °C, respectively, depending on the stiffness of the polymer chain. DSC curves of polyamide **Ic** and **IIc** are shown in Figure S8. The higher T_g in polyamide **I** series could be attributed to the introduction of Me_3TPA moieties, which hindered the rotation of *ortho*-dimethyl-substituted phenyl ring and the movability of the polymer backbone. All the polymers indicated no clear melting endotherms up to the decomposition temperatures on the DSC thermograms, which supports the amorphous nature of these polyamides.

Electrochemical Properties

The electrochemical properties of the polyamides were investigated by CV conducted by film cast on a ITO-coated glass slide as working electrode in anhydrous acetonitrile (CH_3CN) using 0.1 M of TBAP as an electrolyte under nitrogen atmosphere. The typical CV for polyamides **Ib** (with 2,4,6-trimethyl-substituted), **IIb** (with 4-methyl-substituted), and **IIIb** (without substitutions) are shown in Figure 2 for comparison. There is one reversible oxidation redox couples at half-wave potential ($E_{1/2}$) value of 0.91 (E_{onset} = 0.78) V for polyamide **IIIb** (without substitution) in the first oxidation CV scan [Fig. 2(a)]. After scanning for several cycles, a new pair of redox peaks with $E_{1/2}$ at 0.77 and 0.92 V corresponding to TPB structure was observed indicating the formation of 4,4′-diaminobiphenyl linkages (as shown in Scheme 3). The similar observation was also described in our previous study.[28] To prevent the irreversible coupling

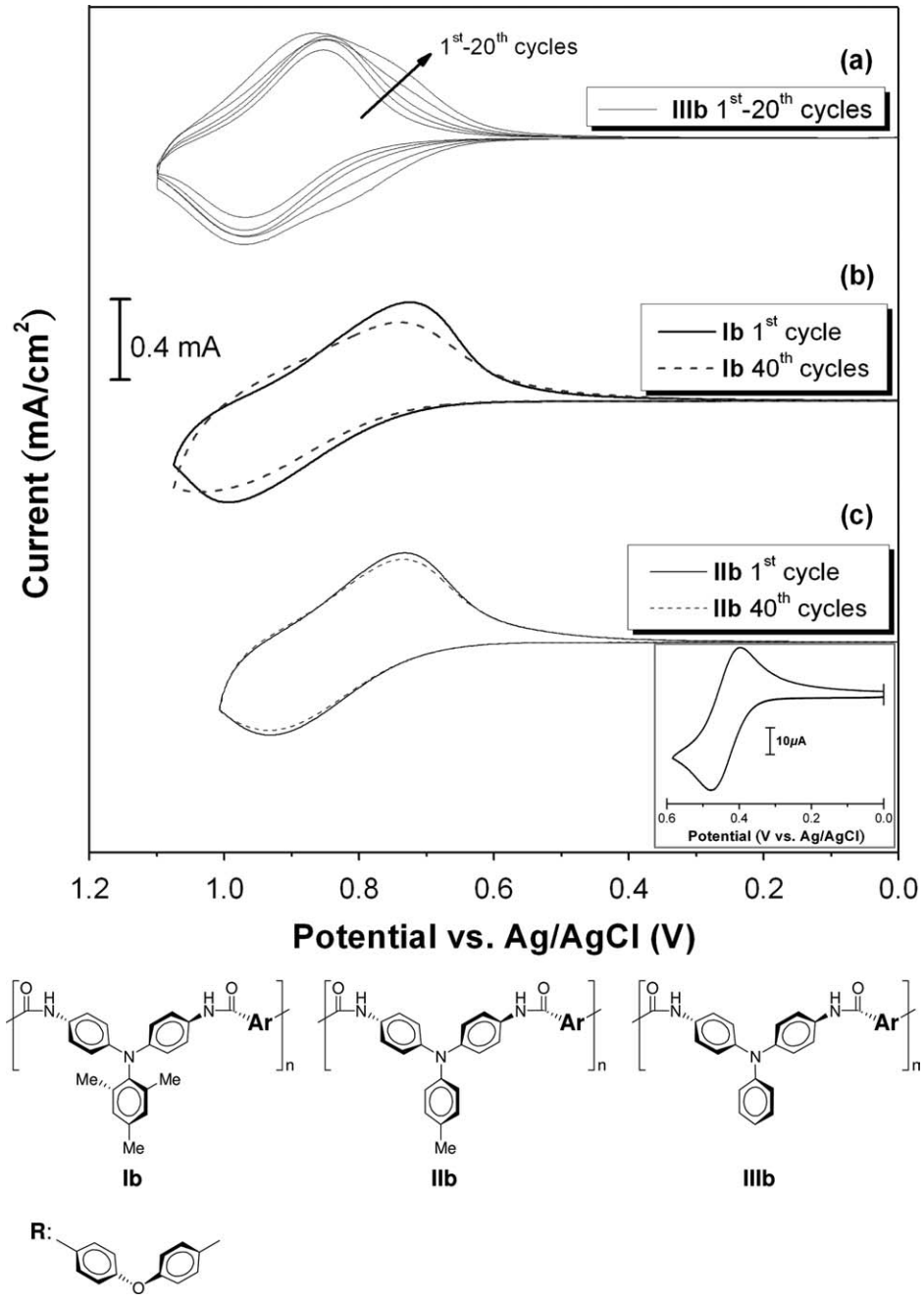

FIGURE 2 Cyclic voltammetric diagrams of polyamide (a) **IIIb**, (b) **Ib**, and (c) **IIb** films on a ITO-coated glass substrate over cyclic scans and ferrocene (inset) in 0.1 M TBAP/CH_3CN at a scan rate of 50 mV/s.

reactions, we tried to design and prepare the polyamides with electron-donating methyl substituents not only at para position but also at ortho position of phenyl rings in a propeller-like TPA geometry. The resulting polyamides showed reversible oxidation redox couples at the $E_{1/2}$ value of 0.89 (E_{onset} = 0.75) V for polyamide **Ib**, and 0.83 (E_{onset} = 0.70) V for polyamide **IIb**, respectively. Both trimethyl- and methyl-substituted TPA structures could effectively prevent the obtained polyamides from taking place irreversible coupling reaction after 40 continuous cyclic scans. However, polyamide **Ib** (with *ortho*- and *para*-methyl protection) gradually lost redox reversibility after more preceding CV scans. On the contrary, the corresponding polyamide **IIb** (with only *para*-methyl protection) still exhibited good electrochemical stability. Furthermore, the Me_3TPA-based polyamides **I** revealed higher oxidation potential than polyamide **II** even though three electron donating methyl groups were attached to the phenyl ring of the Me_3TPA unit. This unexpected phenomenon could be attributed to steric hindrance resulted from the large twisting of the *ortho*-dimethyl-substituted phenyl ring (~77.1°), thus the *n* electrons of the highest occupied molecular orbital (HOMO) on the *N* atom has lower energy level, which means the orbital overlap and electron delocalization between *p*-orbital of *N* atom and π-orbital of Me_3-substituted phenyl ring is low and less resonance when oxidized from its neutral state of Me_3-TPA moiety. The CV

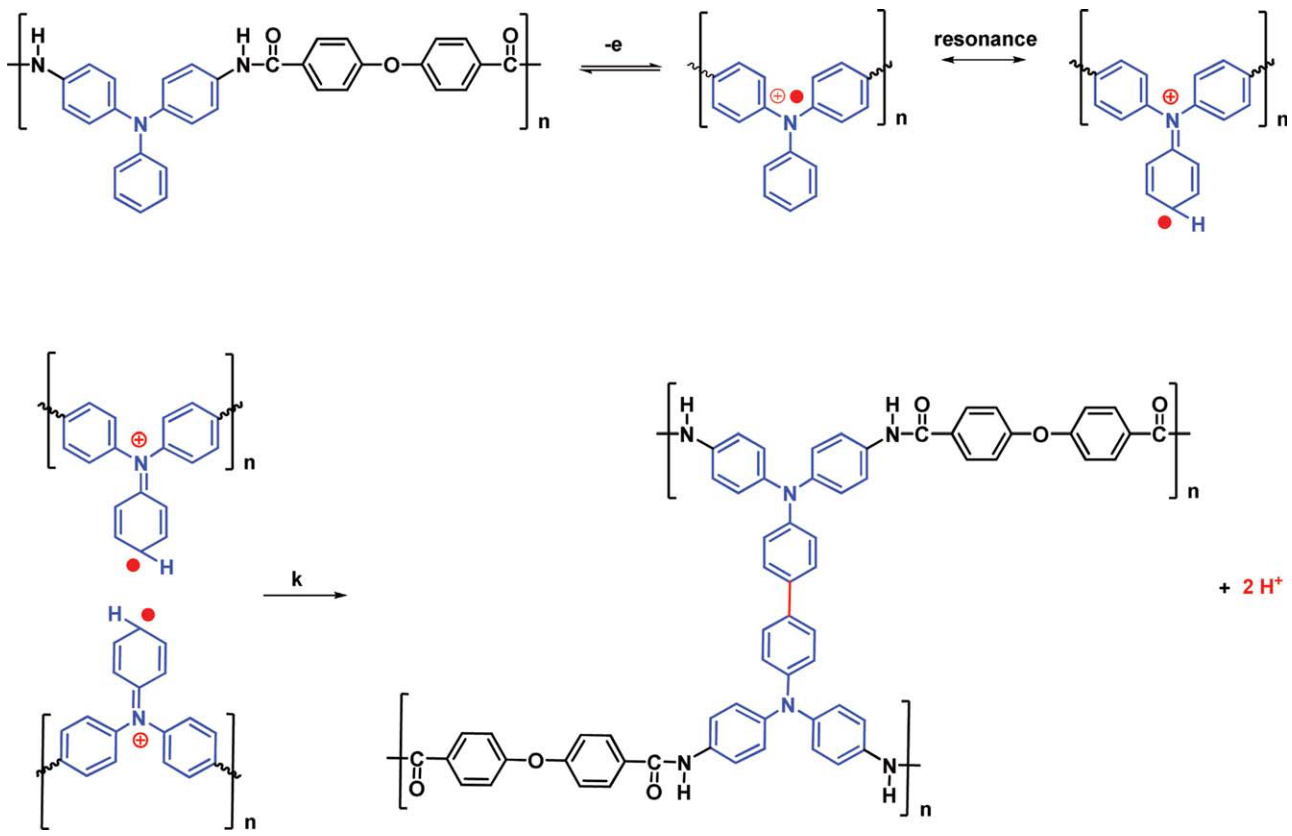

SCHEME 3 TPA-derived polyamide without para-substitution **IIIb** could be dimerized to form TPB moiety by tail to tail coupling. [Color figure can be viewed in the online issue, which is available at wileyonlinelibrary.com.]

curve of polyamide **Ib** with higher oxidative potential was also in agreement with the results of **1** and **M-3Me** (Figure S9), emphasizing the less resonance stabilization of cation radical than that in mono-methyl-substituted polyamide **IIb**. Analog ortho-substitution effect was also mentioned in the literatures.[29,30] The other polyamides showed similar CV curves to that of **Ib** and **IIb**, respectively. The redox potentials of the polyamides as well as their HOMO and lowest unoccupied molecular orbital (vs. vacuum) are shown in Table 1. The HOMO level or called ionization potentials (vs. vacuum) of polyamides **Ia–Ic** and **IIa–IIc** were estimated from the onset of their oxidation in CV experiments as 5.16–5.24 and 5.11–5.19 eV (on the basis that ferrocene/ferrocenium is 4.8 eV below the vacuum level with $E_{onset} = 0.36$ V).

Spectroelectrochemical and Electrochromic Properties

Spectroelectrochemical investigation was used to evaluate the optical properties of the electrochromic materials, and the polyamide film was cast on an ITO-coated glass slide, and a homemade electrochemical cell was built from a

TABLE 1 Redox Potentials and Energy Levels of Polyamides

	Thin Film (nm)		Oxidation Potential (V)[a]				
	λ_{max}	λ_{onset}	$E_{1/2}$	E_{onset}	E_g (eV)[b]	HOMO (eV)[c]	LUMO (eV)
Ia	306	370	0.84	0.72	3.35	5.16	1.81
Ib	338	404	0.89	0.75	3.07	5.19	2.12
Ic	343	413	0.93	0.80	3.00	5.24	2.24
IIa	314	375	0.80	0.67	3.30	5.11	1.81
IIb	343	413	0.83	0.70	3.00	5.14	2.14
IIc	353	423	0.88	0.75	2.93	5.19	2.26

[a] From cyclic votammograms versus Ag/AgCl in CH_3CN. $E_{1/2}$: Average potential of the redox couple peaks.
[b] The data were calculated from polymer films by the equation: $E_g = 1240/\lambda_{onset}$ (energy gap between HOMO and LUMO).
[c] The HOMO energy levels were calculated from cyclic voltammetry and were referenced to ferrocene (4.8 eV; onset = 0.36 V).

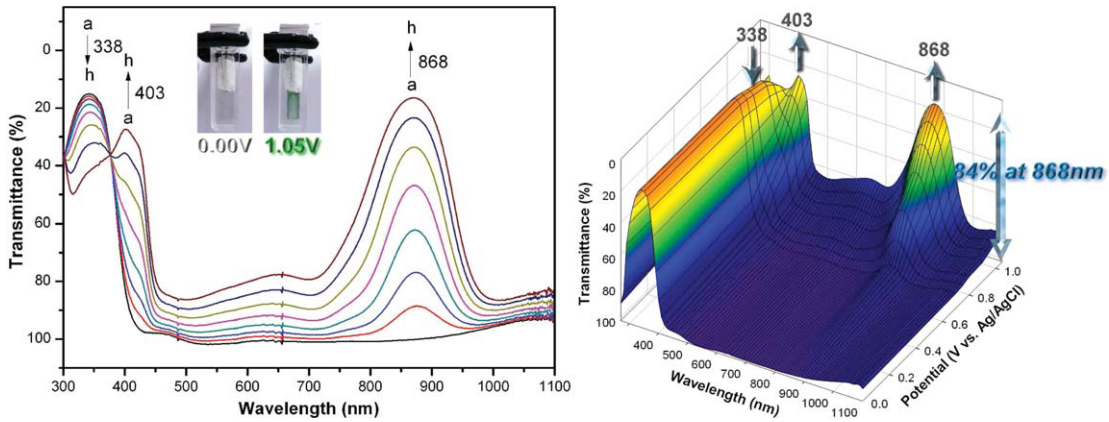

FIGURE 3 Electrochromic behavior (left) at applied potentials of (a) 0, (b) 0.70, (c) 0.75, (d) 0.80, (e) 0.90, (f) 0.95, (g) 1.00, and (h) 1.05 (V vs. Ag/AgCl) and 3D spectroelectrochemical behavior (right) from 0.00 to 1.05 (V vs. Ag/AgCl) of polyamide **Ib** thin film (~120 nm in thickness) on the ITO-coated glass substrate in 0.1 M TBAP/CH_3CN.

commercial UV–vis cuvette. The cell was placed in the optical path of the sample light beam in a UV–vis-NIR spectrophotometer to acquire electronic absorption spectra under potential control in a 0.1 M TBAP/CH_3CN solution. UV–vis-NIR absorbance curves correlated to applied potentials and three-dimensional transmittance-wavelength-applied potential correlation of **Ib** film were depicted in Figure 3. The **Ib** film exhibited strong absorption at ~338 nm, characteristic for TPA unit in the neutral form (0 V) with almost colorless and transparent in the visible region. On oxidation (increasing applied voltage from 0 to 1.05 V), the intensity of the absorption peak at 338 nm gradually decreased while two new peaks grew up at 403 and 868 nm gradually in intensity due to the formation of a stable monocation radical of the Me_3TPA unit. From the inset shown in Figure 3, the polyamide **Ib** film switches from a transmissive neutral form to a highly visible-light absorbing oxidized green form with a high optical transmittance change (ΔT%) of 84% at 868 nm and 58% at 403 nm, respectively. In addition, the spectroelectrochemical behavior of polyamide **IIb** film was shown in Figure 4, and the peak of characteristic absorbance at 343 nm for polyamides **IIb** decreased gradually with increasing applied potential positively from 0 to 1.00 V, whereas new bands grew at 401 and 807 nm additionally. This new spectrum was assigned as that of the monocation radical MeTPA, which revealed the color of bluish-green after oxidation. From the inset shown in Figure 4, the polyamide **IIb** film switches from a transparent neutral state to a highly visible light absorbing oxidized state showing highly optical transmittance change (ΔT%) of 87% at 807 nm and 59% at 401 nm. Besides, the distribution of electrochromic coloration across the polymer film was very homogeneous and stable even after continuous 100 redox cycles. Furthermore, when compared the cutoff wavelengths (absorption edge; λ_{onset}) of polymer films between **Ib** with and **IIb** in neutral state, we observed ~5–10-nm blue shift for polyamide **Ib**, indicating a shorter conjugation length for polyamide **Ib** than **IIb**. Therefore, the possible resonance forms for polyamide **I** and **II** was proposed in Scheme 4.

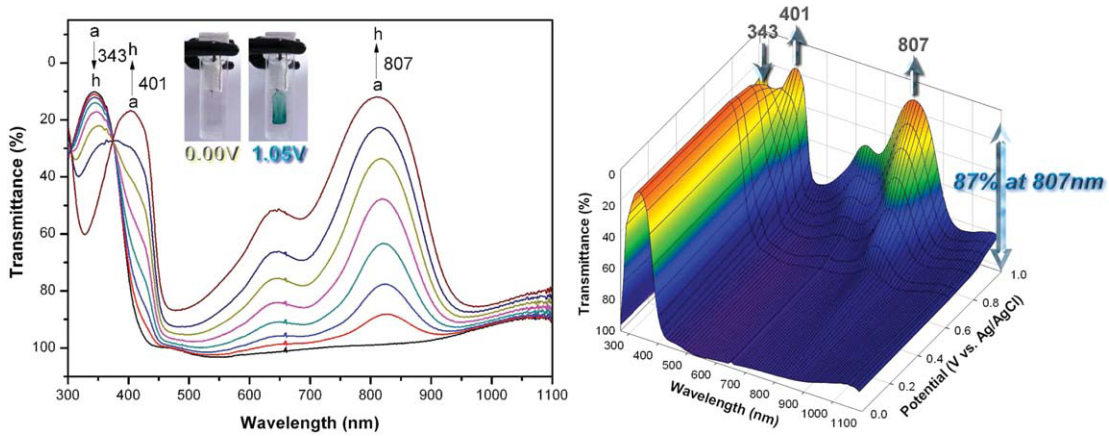

FIGURE 4 Electrochromic behavior (left) at applied potentials of (a) 0, (b) 0.65, (c) 0.70, (d) 0.80, (e) 0.85, (f) 0.90, (g) 0.95, (h) 1.00 (V vs. Ag/AgCl), and 3D spectroelectrochemical behavior (right) from 0.00 to 1.00 (V vs. Ag/AgCl) of polyamide **IIb** thin film (~145 nm in thickness) on the ITO-coated glass substrate in 0.1 M TBAP/CH_3CN.

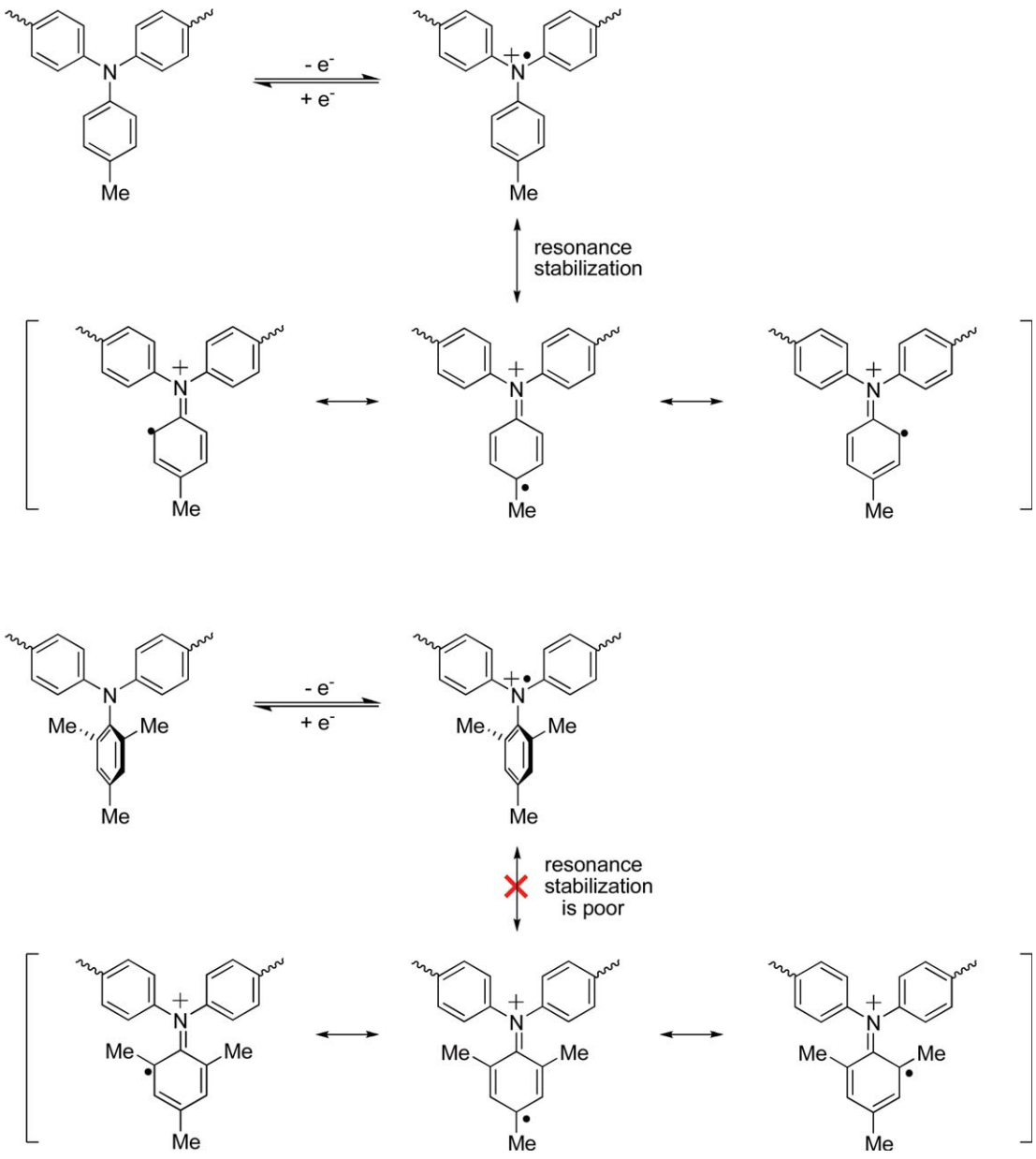

SCHEME 4 Resonance stabilization forms of cation radical of **I** and **II** series. [Color figure can be viewed in the online issue, which is available at wileyonlinelibrary.com.]

The color switching times were estimated by applying a potential step, and the absorbance profiles were followed. The switching time of polyamide **Ib** shown in Figure S10 was defined and calculated as the time required to reach 90% of the full switch absorbance, because it is difficult to perceive any further color change with naked eye beyond this point. The electrochromic stability of the polyamide **Ib** and **IIb** films was determined by measuring the optical change as a function of the number of switching cycles (Fig. 5). The CE ($\eta = \delta OD/Q$) at different switching steps were summarized in Table 2. After continuous 15 cyclic scanning, the polyamide **Ib** film reduced electroactivity gradually. On the contrary, the polymer **IIb** still exhibited good stability of electrochromic characteristics. These results were also consistent in the above-mentioned assumptions of the lower resonance capability due to large twist dihedral angle of inside N_2—C_7 bond in Me_3TPA-based polyamide **I** series.

CONCLUSIONS

Two series of novel organo-soluble and thermally stable electrochromic aromatic polyamides containing electroactive methyl-substituted TPA moieties in the backbone were prepared from the diamine monomers, Me_3TPA-diamine and MeTPA-diamine, with various aromatic dicarboxylic acids, respectively. However, the introduction of more electron-donating methyl groups at ortho position as Me_3-substituted TPA into the polymer main chain could not effectively

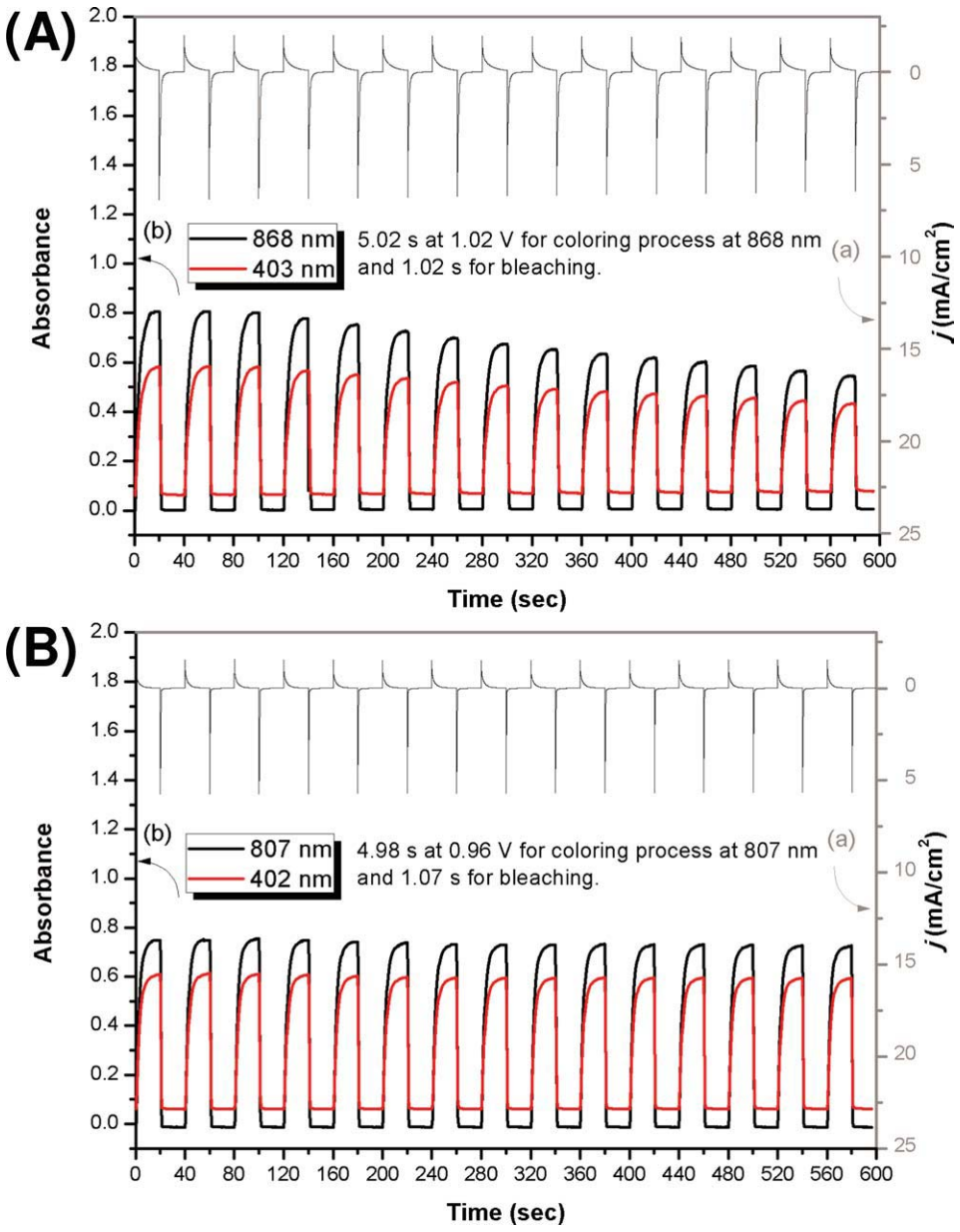

FIGURE 5 Electrochromic switching between (A) 0 and 1.02 V (vs. Ag/AgCl) of polyamide **Ib** thin film (~165 nm in thickness) on the ITO-coated glass substrate (coated area: 1.1 × 0.5 cm^2) and (B) 0 and 0.96 V of polyamide **IIb** thin film (~165 nm in thickness and coated area: 1.0 ×0.5 cm^2) in 0.1 M TBAP/CH_3CN with a cycle time of 40 s. (a) Current consumption and (b) absorbance change monitored at the given wavelength. [Color figure can be viewed in the online issue, which is available at wileyonlinelibrary.com.]

TABLE 2 Optical and Electrochemical Data Collected for Coloration Efficiency Measurements of Polyamides **Ib** and **IIb**

	Ib	**IIb**	Q (mC/cm^2)[c]		η (cm^2/C)[d]		Decay (%)[e]	
Cycling Times[a]	δOD_{868}[b]	δOD_{807}[b]	**Ib**	**IIb**	**Ib**	**IIb**	**Ib**	**IIb**
1	0.808	0.751	5.90	3.34	136	225	0	0
3	0.742	0.751	5.92	3.34	125	225	8.08	0
6	0.662	0.740	5.78	3.30	114	224	16.18	0.44
9	0.594	0.731	5.64	3.29	104	222	23.53	1.33
12	0.542	0.728	5.58	3.27	97	222	28.68	1.33
15	0.503	0.722	5.54	3.27	90	221	33.82	1.78

[a] Switching between 0 and 1.02 for **Ib**, 0 and 0.96 for **IIb** (V vs. Ag/AgCl).
[b] Optical density change at the given wavelength.
[c] Ejected charge, determined from the in situ experiments.
[d] Coloration efficiency is derived from the equation $\eta = \delta OD/Q$.
[e] Decay of coloration efficiency after cyclic scans.

stabilize the cationic radicals of oxidized form comparing with the corresponding polymers with Me-substituted TPA units due to large twist (~77.1°) of N_2-C_7 bond in Me_3TPA structure. The unexpected electrochemical behavior of higher oxidation potential and lower electrochemical stability of Me_3TPA-polyamides **I** than MeTPA corresponding polymers was due to the higher steric hindrance of ortho-substituents in Me_3TPA moieties, thus made the resonance stabilization of cation radical more difficult for the Me_3-substituted phenyl ring.

The authors are grateful to the National Science Council of the Republic of China for financial support of this work, and also to Ting-Shen Kuo of National Taiwan Normal University for giving helps in measuring X-ray single-crystal diffraction.

REFERENCES AND NOTES

1 Monk, P. M. S.; Mortimer, R. J.; Rosseinsky, D. R. Rosseinsky, Electrochromism: Fundamentals and Applications; VCH: Weinheim, 1995.

2 Green, M. Chem Ind 1996, 17, 641–647.

3 Bach, U.; Corr, D.; Lupo, D.; Pichot, F.; Ryan, M. Adv Mater 2002, 14, 845–848.

4 Sonmez, G.; Meng, H.; Wudl, F. Chem Mater 2004, 16, 574–580.

5 Cassidy, P. E. Thermally Stable Polymers, Marcel Dekker, New York, 1980.

6 Yang, H. H. Aromatic High-Strength Fibers; Wiley: New York, 1989.

7 Imai, Y. High Perform Polym 1995, 7, 337–345.

8 Imai, Y. React Funct Polym 1996, 30, 3–15.

9 Hsiao, S. H.; Li, C. T. Macromolecules 1998, 31, 7213–7217.

10 Liou, G. S. J Polym Sci Part A: Polym Chem 1998, 36, 1937–1943.

11 Eastmond, G. C.; Paprotny, J.; Irwin, R. S. Polymer 1999, 40, 469–486.

12 Eastmond, G. C.; Gibas, M.; Paprotny, J. Eur Polym Mater 1999, 35, 2097–2106.

13 Reddy, D. S.; Chou, C. H.; Shu, C. F.; Lee, G. H. Polymer 2003, 44, 557–563.

14 Myung, B. Y.; Ahn, C. J.; Yoon, T. H. Polymer 2004, 45, 3185–3193.

15 Liou, G. S.; Hsiao, S. H.; Ishida, M.; Kakimoto, M.; Imai, Y. J Polym Sci Part A: Polym Chem 2002, 40, 2810–2818.

16 Liou, G. S.; Hsiao, S. H.; Ishida, M.; Kakimoto, M.; Imai, Y. J Polym Sci Part A: Polym Chem 2002, 40, 3815–3822.

17 Liou, G. S.; Hsiao, S. H. J Polym Sci Part A: Polym Chem 2003, 41, 94–105.

18 (a) Hsiao, S. H.; Chen, C. W.; Liou, G. S. J Polym Sci Part A: Polym Chem 2004, 42, 3302–3313; (b) Liou, G. S.; Lin, K. H. J Polym Sci Part A: Polym Chem 2009, 47, 1988–2001; (c) Kung, Y. C.; Liou, G. S.; Hsiao, S. H. J Polym Sci Part A: Polym Chem 2009, 47, 1740–1755; (d) Hsiao, S. H.; Liou, G. S.; Wang, H. M. J Polym Sci Part A: Polym Chem 2009, 47, 2330–2343.

19 (a) Seo, E. T.; Nelson, R. F.; Fritsch, J. M.; Marcoux, L. S.; Leedy, D. W.; Adams, R. N. J Am Chem Soc 1966, 88, 3498–3503; (b) Otero, L.; Sereno, L.; Fungo, F.; Liao, Y. L.; Lin, C. Y.; Wong, K. T. Chem Mater 2006, 18, 3495–3502; (c) Kuorosawa, T.; Chueh, C. C.; Liu, C. L.; Higashihara, T.; Ueda, M.; Chen, W. C. Macromolecules 2010, 43, 1236–1244.

20 (a) Hagopian, L.; Kohler, G.; Walter, R. I. J Phys Chem 1967, 71, 2290–2296; (b) Ito, A.; Ino, H.; Tanaka, K.; Kanemoto, K.; Kato, T. J Org Chem 2002, 67, 491–498.

21 (a) Chang, C. W.; Liou, G. S.; Hsiao, S. H. J Mater Chem 2007, 17, 1007–1015; (b) Liou, G. S.; Chang, C. W. Macromolecules 2008, 41, 1667–1674. (c) Hsiao, S. H.; Liou, G. S.; Kung, Y. C.; Yen, H. J. Macromolecules 2008, 41, 2800–2808; (d) Chang, C. W.; Chung, C. H.; Liou, G. S. Macromolecules 2008, 41, 8441–8451; (e) Chang, C. W.; Liou, G. S. J Mater Chem 2008, 18, 5638–5646; (f) Chang, C. W.; Yen, H. J.; Huang, K. Y.; Yeh, J. M.; Liou, G. S. J Polym Sci Part A: Polym Chem 2008, 46, 7937–7949; (g) Yen, H. J.; Liou, G. S. Chem Mater 2009, 21, 4062–4070; (h) Liou, G. S.; Chang, H. W.; Lin, K. H.; Su, Y. O. J Polym Sci Part A: Polym Chem 2009, 47, 2330–2343.

22 Kvarnström, C.; Petr, A.; Damlin, P.; Lindfors, T.; Ivaska, A.; Dunsch, L. J Solid State Electrochem 2002, 6, 505–512.

23 Wheeler, E. L. U.S. Patent 3,277,174, Oct. 4, 1966.

24 Oishi, Y.; Takado, H.; Yoneyama, M.; Kakimoto, M.; Imai, Y. J Polym Sci Part A: Polym Chem 1990, 28, 1763–1769.

25 Yamazaki, N.; Higashi, F.; Kawabata, J. J Polym Sci Polym Chem Ed 1974, 12, 2149–2154.

26 Yamazaki, N.; Matsumoto, M.; Higashi, F. J Polym Sci Polym Chem Ed 1975, 13, 1373–1380.

27 Su, T. H.; Hsiao, S. H.; Liou, G. S. J Polym Sci Part A: Polym Chem 2005, 43, 2085–2098.

28 Yen, H. J.; Liou, G. S. Org Electron 2010, 11, 299–310.

29 Nishiumi, T.; Nomura, Y.; Chimoto, Y.; Higuchi, M.; Yamamoto, K. J Phys Chem B 2004, 108, 7992–8000.

30 Wang, B. C.; Liao, H. R.; Chang, J. C.; Chen, L.; Yeh, J. T. J Lumin 2007, 124, 333–342.